



1 **Attributing Regional Trends of Evapotranspiration and Gross**
2 **Primary Productivity with Remote Sensing: A case study in the**
3 **North China Plain**

4
5 Xingguo Mo^{1,2}, Xuejuan Chen^{1,2}, Shi Hu¹, Suxia Liu^{1,2}, Jun Xia¹

- 6
7 1. Key Laboratory of Water Cycle & Related Land Surface Processes, Institute of
8 Geographic Sciences and Natural Resources Research, Chinese Academy of Sciences,
9 Beijing 100101, China.
10 2. University of Chinese Academy of Sciences

11
12 Correspondence to: Xingguo Mo, E-mail: moxg@igsnr.ac.cn

13
14 **Abstract**

15 Attributing changes of evapotranspiration (ET) and gross primary productivity (GPP) are
16 crucial for impacts and adaptation assessment of the agro-ecosystems to climate change.
17 Simulations with VIP model revealed that annual ET and GPP were slightly increasing from
18 1981 to 2013 over the North China Plain. The tendencies of both ET and GPP were upward in
19 spring season, while the trends are weak and downward in summer season. A complete
20 factor - separation analysis illustrated that the relative contributions of climatic change, CO₂
21 fertilization and management to ET (GPP) trend were 56 (-32)%, -28 (25)% and 68 (108)%,
22 respectively. The decline of global radiation resulted from deteriorated aerosol and air
23 pollution was the principal causes of GPP decline in summer, while air warming intensified
24 the water cycle and advanced the plant productivity in the spring season. Agronomical
25 improvements were the principal drivers of crop productivity enhancement.

26
27 Key words: Climate change; Contribution; VIP model; Evapotranspiration; Gross primary
28 productivity

29 **1. Introduction**

30 Terrestrial hydrological and carbon cycles are intimately coupled via transpiration and



31 photosynthesis processes which are regulated by plant leaf stomata. Due to land use/cover
32 changes, intensified agricultural management and climatic change, terrestrial
33 eco-hydrological processes have been noticeably shifted at multiple spatiotemporal scales
34 (Tian et al., 2011; Douville et al., 2013), for example, prevailing irrigation and application of
35 chemical fertilizers have raised soil moisture, evapotranspiration (ET) and crop productivity,
36 etc. In some regions the effects of human activities are the same magnitude as, or even exceed
37 the impacts of global warming on the productions of agro-ecosystems (Haddeland et al.,
38 2014). In the last decades, global consumptive water use and carbon fixation by terrestrial
39 ecosystems are demonstrated to be slightly increasing with more efficient water use,
40 corresponding to changes of climatic factors and fertilization effect of elevated atmospheric
41 CO₂ concentration (Yan et al., 2013; Nayak et al., 2013). Spatiotemporal patterns of water
42 and carbon fluxes at regional scale are changing under global change (Zeng et al., 2014; Liu
43 et al., 2012).

44 As ET being the major component of water budget in the water limited basins, its long
45 term tendency has been taken as an indicator for diagnosing the intensification of regional
46 water cycle. The complementary relationship between actual and potential ET may reveal
47 some clues of hydrological changes. Observations in the last decades illustrated that potential
48 evaporation rates (ET_p)(represented as pan evaporation) were decreasing in Europe, U.S.,
49 China, India, Australia (Brutsaert, 2006; Katul et al., 2012), implicating the decline of
50 available energy and aerodynamics devoted to latent heat flux over the land surface. The
51 climatic factors dominating ET_p change are usually diverse. For example, over the North
52 China Plain (NCP) the changes of ET_p were mainly attributed to declines of global radiation
53 and near surface wind speed (Tang et al., 2011; Song et al., 2010). However, in southern
54 Turkey a noticeable decline of ET_p was attributed to enhanced air humidity associated with
55 the expansion of irrigation acreage and more water evaporated into the atmospheric boundary
56 layer (Ozdogan and Salvucci, 2004). Burn and Hesch (2007) revealed that decreasing wind
57 speed and raised water vapor deficit were responding to trend of ET_p in Canadian Prairies. At
58 large scale, precipitation is usually the principal factor determining actual ET changing, such
59 as Qian et al. (2007) presented that increase of ET in the Mississippi River basin was
60 following precipitation propensity, while the effects of solar radiation and air temperature



61 changes were minor.

62 Terrestrial eco-hydrological processes are driven by climate and modulated by human
63 activities. Generally climate warming enhances atmospheric evaporative demand, while CO₂
64 fertilization stimulates photosynthesis and inhibits leaf stomatal conductance, leading to more
65 biomass accumulation and higher water productivity (Field et al., 1995; Buckley and Mott,
66 2013). Simultaneously, land use change and land management also noticeably affect the
67 ecosystem production and hydrological fluxes (Shi et al., 2011). Separating the contributions
68 of climatic change, CO₂ enrichment and human activities to the long term trends of water and
69 carbon cycles is critical for assessment of ecosystem responses and resilience to
70 environmental changes. Some researchers have explored the relative contributions of climate
71 change and vegetation dynamics to changes of global land surface evapotranspiration and
72 river runoff (Betts et al., 2007; Piao et al., 2007; Alkama et al., 2010; Liu et al., 2012; Chen et
73 al., 2014; Banger et al., 2015), but the conclusions are inconsistent yet. Climate change
74 dominated the inter-annual variability of ET, while land use changes and agricultural practices
75 and techniques exerted more discernable effects on water cycle in long term (Liu et al., 2012).
76 However, Alkama et al. (2010) and Shi et al. (2011) demonstrated that climate change is the
77 predominant driver of the changes of global ET in 20th century. For the contributions of
78 climate change to vegetation productivities at large scale may be explored by ecosystem
79 models or statistical models. Piao et al. (2015) documented that elevated atmospheric CO₂
80 and nitrogen deposition were the critical contributors to terrestrial greening over China in the
81 last three decades; Baker et al. (2010) figured out that climate anomalies in springtime were
82 the most frequent drivers to annual GPP variability in the North America; Nayak et al. (2013)
83 reported that climate change had a relatively small but significant control (15%) on the trend
84 of terrestrial net primary production (NPP) over India during 1981 to 2005. In the crop
85 ecosystems, contributions of climate change, cultivar renewal and agronomic management to
86 change of crop yield have been separated with crop or statistical models (Yu et al, 2012; Song
87 et al., 2014; Bai et al., 2015; Guo et al., 2014; Wang Z. et al., 2016). The impacts of climate
88 change on crop yield may be positive or negative in different regions, depending on the
89 tendencies of the dominant factors (Ewert et al., 2015).

90 As one of the granaries in China, North China Plain (NCP) is experiencing challenges of



91 agriculture sustainability due to global change and social development. Thereby, it is crucial
92 to understand the impacts of climate change on the productions of cropping systems. Over the
93 plain, winter wheat – summer maize double cropping system is prevailing, supported by
94 irrigation, fertilizer and agronomical techniques. *In situ* measurements, agricultural annals and
95 regional remotely sensed vegetation index dataset all illustrated that both wheat and maize
96 productivities have enhanced remarkably during the last three decades (Yuan and Shen, 2013);
97 correspondingly, the seasonal water consumption and water use efficiency are also slightly
98 improved (Zhang et al., 2011). The achievement of long term increasing grain production is
99 related to the active adoption of new varieties for stabilizing, extending the length of crop
100 growth period, as well as agronomical technique advancement (Liu et al., 2010; Sacks and
101 Kucharik, 2011). Currently, water amount for food production is consisted of 65% of total
102 water consumption here. Further, along with the gradually augmented domestic and industrial
103 water requirement, groundwater in some parts of the plain has been over-exploited, and the
104 environmental water requirement is generally under deficit conditions (e.g., MWR, 2010).
105 Facing with the rapid deteriorating agricultural environment, some critical issues are still
106 unclear, such as, what mechanisms drive the evolutions of eco-hydrological processes over
107 this plain? What are the impacts of climate change on the cropping systems?

108 In this study, the VIP eco-hydrological dynamic model integrated with NOAA-AVHRR
109 remotely sensed normalized difference of vegetation index (NDVI) is employed to assess the
110 spatiotemporal evolutions of ET and vegetation GPP over the NCP during 1981 to 2013. By
111 numerical experiments with the VIP model and the factor separation method, the
112 contributions of climate change, fertilization of atmospheric CO₂ enrichment and agronomical
113 practices and technological advancement to crop water consumption and productivity are then
114 analyzed, and the relevant mechanisms are discussed.

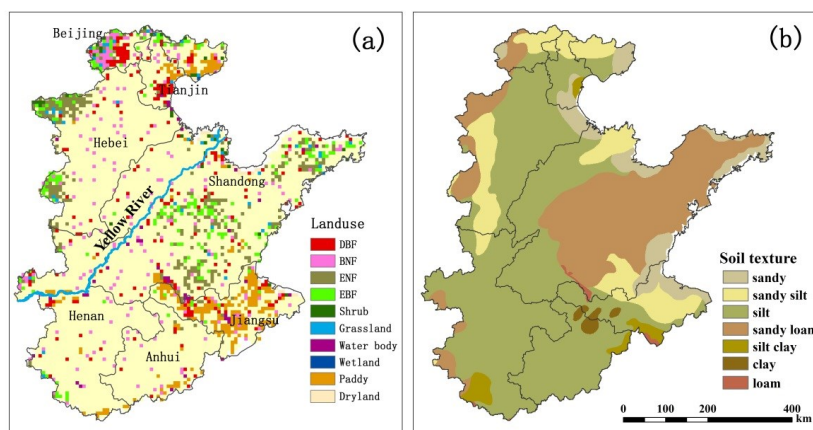
115 **2. Method and materials**

116 **2.1 Study site**

117 The NCP is one of the country's granaries, extending from latitude 32°00' to 40°24'N
118 and longitude 112°48' to 122°45'E (Fig. 1(a, b)). It is located in the eastern part of China with



119 an area of $33 \times 10^4 \text{ km}^2$, which is an alluvial plain developed by the intermittent flooding of the
120 Huang, Huai and Hai Rivers and 72% is cultivated as farmland. The warm temperate climate
121 varies gradually from sub-humid in the southern to semi - arid in the northern parts. The
122 annual precipitation ranges from 500 - 1000 mm, occurring irregularly among seasons and
123 more than 70% falls in summer. Soil moisture deficit happens widely during the the spring
124 and early summer period. Besides soybean/millet/sorghum/cotton, the double cropping
125 system of winter wheat - summer maize is prevailing in the plain, where wheat and maize are
126 the most common harvest crops in summer and autumn seasons, respectively. Due to
127 insufficient precipitation, the spring crops (such as wheat) usually need supplemental
128 irrigation to form favorable production.



129

130

131 Fig. 1 Land use/cover (a) and soil texture (b) of the North China Plain (NCP) (DBF:
132 Deciduous Broadleaf Forest; BNF: Broadleaf and Needle leaf Mixed Forest; ENF: Evergreen
133 Needle leaf Forest; EBF: Evergreen Broadleaf Forest)

134

135 2.2 The VIP eco-hydrological Model

136

137 The physically process-based VIP (Vegetation Interface Processes) eco-hydrological model
138 is designed to simulate the exchanges of energy, water and carbon between terrestrial
139 ecosystem and atmosphere (Mo et al., 2014). In the model, ET is termed as the summation of
140 canopy transpiration, evaporation from canopy intercept and soil surface, computed
141 separately with the Penman-Monteith Equation. Transpiration and photosynthesis processes



142 are coupled through the Ball-Berry relationship between leaf stomatal conductance and net
143 assimilation rate. On carbon cycle aspect, leaf carbon fixations on sunlit and shaded leaves
144 groups are predicted with the biochemical schemes for C3 (Farquhar et al., 1980) and C4
145 plants (Collatz et al., 1992). In the radiation budget scheme, shortwave radiation transfer in
146 canopy distinguishes the leaf spectral properties of visible and near infrared radiation, as well
147 as fraction of direct beam and diffusive irradiance in global radiation. Precipitation
148 throughfall - runoff generation over the land surface is calculated with a curve - number (CN)
149 type equation at daily scale, using the daily net precipitation and the moisture deficit of
150 upper-soil layer in this study. Simulation of soil water movement in root zone is carried out
151 with a discrete Richards Equation in three layers. The crop and natural vegetation growth
152 modules are also embedded in the model to simulate the biomass mass accumulation and
153 carbon cycle.

154 **2.3 Data**

155 The VIP model input data include land use/cover, soil physical properties, and atmospheric
156 forcing variables. GIMMS AVHRR 15-day normalized difference of vegetation index time
157 series (NDVI3g) from 1981 to 2013 is used to retrieve the vegetation leaf area index and
158 other land surface characteristics ([https://nex.nasa.gov/nex/projects/1349/wiki/general_data_](https://nex.nasa.gov/nex/projects/1349/wiki/general_data_description_and_access/)
159 [description_and_access/](https://nex.nasa.gov/nex/projects/1349/wiki/general_data_description_and_access/)) (Pinzon and Tucker, 2014). The land use classification is originated
160 from both Landsat TM images (www.geodata.ac.cn) and MODIS remote sensing products, in
161 which the farmland is classified as rice paddy and dryland. Soil textural data are at a scale of
162 1:1,000,000 represented as fractions of sand, silt and clay, by which the parameters of soil
163 porosity (θ_{sat}) and saturated hydraulic conductivity (K_{ws} , mm s^{-1}) are estimated as Bonan
164 (1996). Daily climate variables (air temperature, water vapor pressure, wind speed, sunshine
165 duration and precipitation) recorded at 87 climatic stations (<http://cdc.cma.gov.cn/>) in and
166 around the study area are available for generating the spatial atmospheric forces. The NDVI
167 data are error-checked and the erroneous data are replaced by interpolation with the preceding
168 and subsequent values according to the time series by the Savitzky–Golay (SG) filter
169 (Savitzky and Golay, 1964), and then the daily values are derived with the Lagrange
170 polynomial. Vegetation leaf area index (LAI) is retrieved from NDVI with empirical



171 relationships for different plant function types.

172 The data used for model validation are field flux measurements with eddy covariance
173 technique at Yucheng (116°38'E, 36°57'N), Daxing (116°25'E, 39°37'N), Miyun (117°19'E,
174 40°38'N) and Guantao (115°8'E, 36°31'N) sites over the plain. The cropping systems at the
175 Yucheng, Daxing and Guantao sites are all rotations of winter wheat – summer maize, while
176 land cover is dwarf shrub at the Miyun site. The eddy covariance data are processed with
177 general procedures (Liu and Xu, 2013). GPP data are available only at Yucheng site. In
178 addition to the eddy fluxes, grain yield records of wheat and maize in county statistics are also
179 used to verify the GPP predictions at regional scale.

180 **2.4 Model implementation and experimental design**

181 **2.4.1 Simulation setup**

182 The model simulations were conducted at 8 - km spatial resolution and half - hour time step.
183 The cropland is classified into wheat and maize or rice double cropping systems. Atmospheric
184 driving forces are interpolated from daily meteorological variables recorded at the climatic
185 stations to grid cells with a gradient inverse distance square method (GIDS), which accounts
186 for the effects of elevation, latitude and longitude (Nalder and Wein, 1998). Estimated with
187 sunshine duration in a linear relationship, the global radiation is subdivided into direct visible
188 and near infrared parts, as well as direct beam and diffusive components with Weiss and
189 Norman (1985). The daily air temperature is extended to hourly values with a sinusoid
190 function based on the daily maximum and minimum temperatures (Cambell and Norman,
191 1998). During the winter wheat growing period, irrigation water is supplied when water
192 storage in the root zone is below 60% of the field capacity. Summer maize is set to be
193 irrigated not more than one time in its growth period. The simulation is conducted with
194 prescribed daily LAI series retrieved from remotely sensed NDVI series for eco-hydrological
195 prediction from 1980 to 2013, in which the first year is taken as warming up.

196 **2.4.2 Separation of the contributions of climate change and management effects**

197 By using a general function, f , the scalar fluxes (water vapor and carbon) between land



198 surface and the atmosphere are determined by climate factors (M), atmospheric CO_2
 199 fertilization (C) and agronomical management and technological advancement (In this study
 200 we assume the long term trend of leaf area index (LAI) may represent the effects of human
 201 activities on ecosystems of crop and natural ecosystems. Human activities to the
 202 agro-ecosystem include renewals of cultivars, irrigation facility improvement, fertilizer use
 203 application, soil quality amelioration, etc.), namely,

$$204 \quad f = F(M, C, LAI, \dots) \quad (1)$$

205 The changes of f contributed by a single factor (expressed as f_i) and its interaction with
 206 another factor (expressed as f_{ij}) can be decomposed by the Taylor expansion as,

$$207 \quad f_i = \frac{\partial F}{\partial x_i} \Delta x_i + \frac{1}{2!} \frac{\partial^2 F}{\partial x_i^2} \Delta x_i^2 + \dots + \frac{1}{n!} \frac{\partial^n F}{\partial x_i^n} \Delta x_i^n \quad (2)$$

$$208 \quad f_{ij} = f_i + f_j + \frac{\partial^2 F}{\partial x_i \partial x_j} \Delta x_i \Delta x_j + \dots \quad (3)$$

209 where x_i and x_j ($i \neq j$) represent M , C and LAI , respectively. The factor separation methodology
 210 from Stein and Alpert (1993) and Alkama et al. (2010) is used to category the contributions of
 211 climate change, CO_2 fertilization and LAI , and their interactions to long term trends of ET and
 212 GPP. Similar to Alkama et al. (2010), the total effect, f_{123} , is expressed as,

$$213 \quad f_{123} = f_1 + f_2 + f_3 + f^{12} + f^{13} + f^{23} + f^{123} \quad (4)$$

214 With

$$215 \quad f^{12} = f_{12} - f_1 - f_2 \quad (5)$$

$$216 \quad f^{13} = f_{13} - f_1 - f_3 \quad (6)$$

$$217 \quad f^{23} = f_{23} - f_2 - f_3 \quad (7)$$

218 Where f_1 , f_2 and f_3 are the direct contributions of climate change, atmospheric CO_2 enrichment
 219 fertilization and agronomical management, respectively; f^{12} is the contribution of interactions
 220 of climate change and CO_2 enrichment; f^{13} is the contribution of interactions between climate
 221 change and management; f^{23} is the contribution of interactions between CO_2 fertilization and
 222 agronomical management; f^{123} is the contribution of interactions between climate change, CO_2
 223 fertilization and agronomical management.

224 Seven numerical experiments designed to fully distinguish the contributions of climate
 225 change, CO_2 fertilization and agronomical management are conducted by the VIP model over
 226 the NCP from 1981 to 2013. The experiments are as following:



- 227 (1) f_{123} (“all factors”): Current climate, CO₂ and LAI spatiotemporal pattern;
- 228 (2) f_1 (“climate change effect”): Current climate, but atmospheric CO₂ concentration is fixed
229 at year 1981, and LAI pattern is set as the multi-year average;
- 230 (3) f_2 (“CO₂ fertilization effects”): Climate and LAI fixed at a specific year, but current CO₂
231 concentration;
- 232 (4) f_3 (“management effect”): Climate and CO₂ concentration are fixed a specific year, but
233 current LAI pattern is used;
- 234 (5) f_{12} (“climate change and CO₂ fertilization effects”): LAI pattern is fixed, but current
235 climate and CO₂ concentration are used;
- 236 (6) f_{13} (“climate change and management effects”): CO₂ concentration is fixed, but current
237 climate and LAI pattern are used;
- 238 (7) f_{23} (“CO₂ fertilization and management effects”): Climate is fixed at 1981, but current
239 CO₂ and LAI are used.
- 240 The trends of annual ET and GPP in the above experiments are calculated. According to
241 Eq.(4) to Eq.(7), the contributions of climate change, CO₂ fertilization and management to ET
242 and GPP long term trends are separated.

243 **3. Result analysis**

244 **3.1 Model Verification**

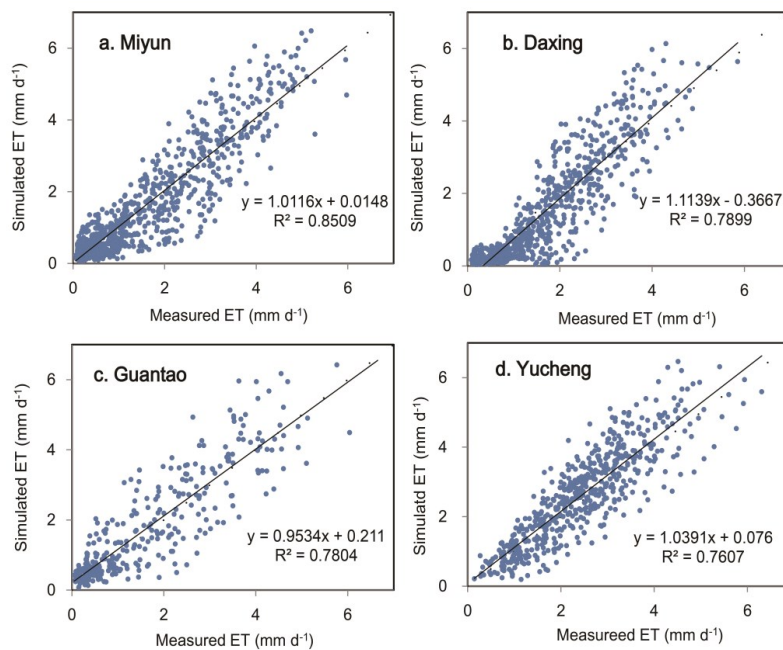
245 **3.1.1 Validated with eddy covariance measurements**

246 The VIP model is used to simulate the hydrological, energy partitioning and crop growth
247 processes at the four sites of eddy flux measurement. Here, eddy covariance measurements of
248 daily ET and GPP are employed to verify the model predictions (ET is available in all the
249 sites, but GPP is only available at one site). The land surface characteristics are relatively
250 homogeneous surround the measuring sites, ensuring the footprint for measured fluxes. The
251 meteorological information measured at each site is used to drive the VIP model. It is shown
252 that the agreements are quite satisfactory for both ET and GPP (Fig.2 and Fig.3). Totally, there



253 are 9-year daily ET data and 3-year daily GPP data for comparison with the model
254 simulations. The coefficients of determination (R^2) are above 0.76 for all the sites. At annual
255 scale, the absolute relative biases of predicted ET are ranged from 1.5 to 12.6% in the 9-year
256 dataset, and biases of GPP are from 2.0 to 8.8% in 3-year data. Therefore, the model
257 performance is quite well and reliable for vegetation/crop productivity and water consumption
258 predictions. The biases may be stemmed from both measurements and model uncertainty. Mo
259 et al. (2012) showed that the canopy leaf area index (LAI) and photosynthetic capacity
260 (carboxylation rate for C3 crops and photon quantum use efficiency for C4 crops) were the
261 most sensitive parameters to the model efficiency. Here, taking Yucheng site as an example,
262 annual ET and GPP may increase 1.6% (2.6%) and 3.0% (15.9%) respectively as LAI
263 (photosynthesis capacity) is increased by 20%.

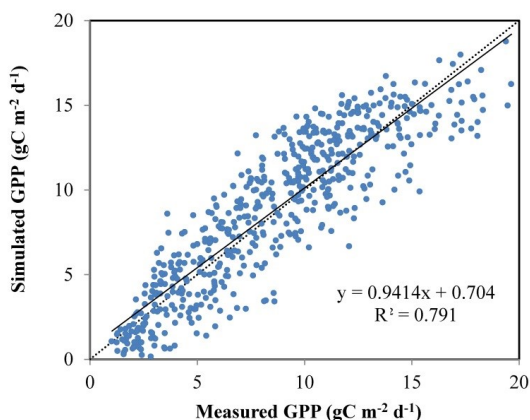
264



265

266 Fig.2 Comparison of the simulated daily ET and GPP with the eddy covariance

267 measurements



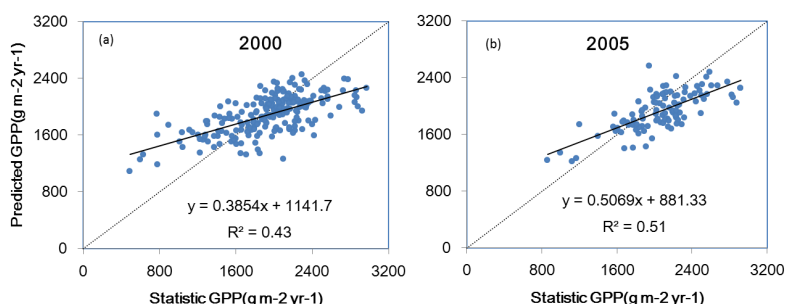
268

269 Fig.3 Comparison of the simulated GPP with eddy covariance measurements at the Yucheng
270 site

271 3.1.2 Validated with the statistical yield records

272 The simulated GPP is also validated with the statistic staple crop grain yields at county
273 level. The yield per hectare is converted to equivalent GPP per square meter. As shown in
274 Fig.4 (years of 2000 and 2005 are used), the agreement is satisfactory with the coefficient of
275 determination (R^2) of 0.43 and 0.51 ($p < 0.001$), respectively. There are remarkable spatial
276 variations of crop yields resulted from diverse conditions of climate, soil and management. In
277 the simulation, it is found that the spatiotemporal evolution of greenness is the dominant
278 factor of yield patterns. Greenness represented by the vegetation index is an appropriate
279 indicator of crop productivity under environmental stresses (Hu et al., 2014). In the areas with
280 high vegetation index and favorable irrigation facilities, the yield losses may be caused by
281 heat waves or pest infections in the maturity stage.

282



283

284 Fig.4 Comparison of the predicted GPP and statistic yield derived GPP at county scale in
285 2000 and 2005.

286

287 3.2 Trends of climate, crop productivity and ET

288 Changes of climate variables and agro-ecosystem management are the dominant driving
289 forces for evolution of regional eco-hydrological processes. Intra-seasonal variations of
290 climatic variables may exert different impacts on the crop water consumption and carbon
291 assimilation. In the last three decades, air temperature is rising, but sunshine duration and
292 wind speed are decreasing significantly over the plain, associated with global climate change,
293 aerosol and air pollutions. Soil amelioration, genetic improvement, irrigation facility
294 constructions and application of chemical synthesis fertilizer are considered to be the
295 principal factors that have propelled productictiy close to the attainable level(Yu et al., 2012;
296 Lobell and Burke, 2010).

297 3.2.1 Changes of climatic variables

298 Grid averages of the climatic variables were interpolated with GIDS (Gradient Inverse
299 Distance Square) method over the North China Plain from 1980 to 2013. Nevertheless
300 inhomogeneous distributions of the climatic variables, the spatially averaged trends were
301 clear (Table 1). At annual scale, global radiation, air temperature (especially minimum
302 temperature) and wind speed were significantly changing ($p < 0.01$). At monthly scale,
303 radiation was declining in all the months except March, but only trends in June to September
304 were significant ($p < 0.01$); Significant increasing of air temperature is occurred in spring
305 (February and March) and early summer (May to July); Wind speed was decreasing



306 significantly ($p < 0.01$) in all the months except August. However, no significant trends were
 307 detected for both precipitation and water vapor pressure throughout each month. As a
 308 consequence, water vapor pressure deficit was exaggerated along with the rising of air
 309 temperature, which was expected to intensify the atmospheric water vapor demand and offset
 310 the negative effects of declining radiation and wind speed on potential evaporation). These
 311 changes in climatic variables have exerted remarkable impacts on the crop phenological
 312 stages, water consumption and productivity during the last three decades over the North
 313 China Plain (Liu et al., 2010).

314

315 Table 1. Inter-annual trends of monthly sunshine duration, precipitation, air temperature, relative
 316 humidity and wind speed (Significant levels: * for $p < 0.05$; **for $p < 0.01$).

317

	Jan	Feb	Mar	Apr	May	Jun	Jul	Aug	Sept	Oct	Nov	Dec
Sun(h/yr)	-0.026	-0.036*	0.015	-0.012	-0.015	-0.039**	-0.040**	-0.052**	-0.060**	-0.018	-0.017	-0.020
P(mm/yr)	-0.129	0.212	-0.279	0.354	0.049	-0.472	0.608	0.456	0.694	-0.706	0.223	0.084
T(°C/yr)	0.022	0.058*	0.078**	0.030	0.042**	0.029*	0.030*	0.017	0.020	0.044*	0.025	0.018
rh(%/yr)	-0.065	0.115	-0.260*	-0.079	-0.139	-0.074	-0.080	-0.074	0.057	-0.125	-0.094	-0.091
U(m/s/yr)	-0.016**	-0.012**	-0.012**	-0.020**	-0.021**	-0.019**	-0.015**	-0.006	-0.014**	-0.017**	-0.015**	-0.012**

318

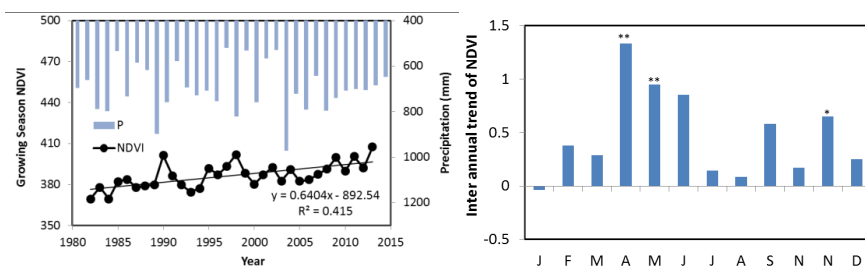
319 3.2.2 Changes of Greenness and GPP

320 Here remotely sensed NDVI is expressed as vegetation greenness. Averaged over the
 321 growth period (from March to October), vegetation greenness was significantly increasing
 322 from 1980s with a trend of 0.64/yr ($p < 0.001$) and coefficient of variation (CV) of 2.4%
 323 (Fig.5(a, b)). It was noted that the maximum inter-annual variation of greenness was 5.4%
 324 between two consecutive dry and wet years (1989 and 1990) with 280 mm difference of
 325 annual precipitation. The distinguish differences of greenness occurred in June to December.
 326 At annual scale greenness was weakly related with precipitation; however, in growing season,
 327 greenness was noticeably correlated with monthly precipitation in April, May, June,
 328 September and November ($r = 0.29 \sim 0.53$, $p < 0.1$). The reason is that the monthly rainfall is

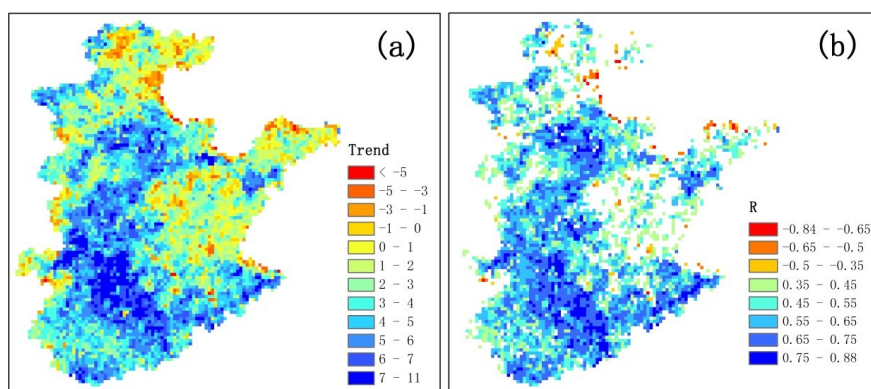


329 generally lower than the atmospheric evaporative demand in spring season, and the water
 330 deficit to transpiration generally stresses the plant growth. Unlike precipitation, greenness
 331 anomalies are positively correlated with the detrended air temperature ($r^2=0.16$, $p<0.05$),
 332 implicating that recent climate warming has stimulated vegetation growth through extending
 333 the growing stage and through pushing photosynthesis in water no-limited regions (Mao et
 334 al., 2012; Nemani et al., 2003).

335 Regional greenness trends showed remarkably diverse (Fig.6(a, b)). Except climate change,
 336 human activities also exerted critical impacts on the land greenness variations. In the low
 337 plain of Hebei province, saline - alkali land amelioration and irrigation facilities improvement
 338 have contributed greatly to the greenness enhancement in the 1980s to 1990s. In addition,
 339 atmospheric nitrogen deposition was also regarded as a positive driver for the land greening,
 340 since the nitrogen deposition has averagely increased by 25% from 1990s to 2000s in North
 341 China (Jia et al., 2014; Piao et al., 2015). Spatially, greenness over 91.3% of the NCP was
 342 increasing, in which the most distinctive grids distributed in the southern parts and the belt
 343 along the yellow river channel, where water supply was usually sufficient. In the northern part,
 344 tendencies of greenness in a number of grids were decreasing significantly at $p=0.1$ level,
 345 which were resulted from less irrigation supply to farmland in springtime and rapid expansion
 346 of built-up occupations around cities and towns, such as Beijing and Tianjin metropolitans.



347
 348
 349 Fig.5 Spatial average trends of growing season NDVI at annual (a) and monthly scales (b)
 350 (Significant levels: * is $p<0.05$; ** is $p<0.01$).
 351



352

353

354 Fig.6 (a) Spatial distributions of NDVI trend in growing season and (b) the Pearson
355 coefficients of NDVI trend above $p < 0.05$ significant level
356

357

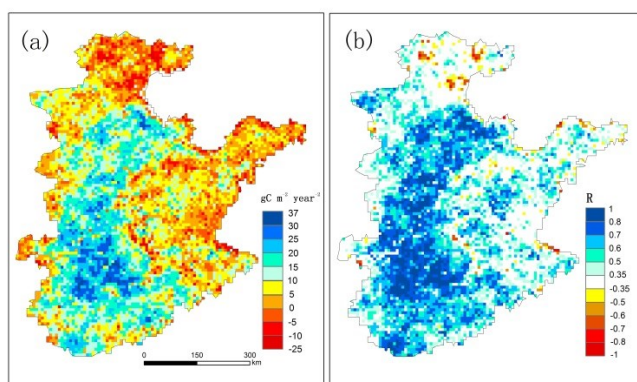
358 The spatially averaged GPP was $1913 \pm 584 \text{ gC m}^{-2} \text{ yr}^{-1}$ with CV of 6.8% predicted by the
359 VIP model from 1981 to 2013, showing great spatial variability (Fig.7). Low crop
360 productivity was resulted from fields with saline-alkali soil in the low lands nearby the coast
361 of Bohai Sea, where almost no favorable water was available for irrigation purpose in
362 springtime. Averagely, the increasing trend of GPP was significant with a slope of 8.2 gC m^{-2}
363 yr^{-2} ($r=0.60$, $p < 0.01$). It was noticed that the average annual GPP was increasing steadily from
364 1980s to 2000s, compounded by decadal variations of the climate and elevated atmospheric
365 CO_2 , as well as the improvement of agricultural practices and techniques. Trends of annual
366 GPP were positive over 87.9% of the study region. As shown in Fig.7, the obvious increasing
367 trends were located in the mid and southern areas, while most of the decreasing trends
368 occurred in the eastern and northern parts, where water for irrigation was considerably
369 reduced in spring season because of competing demand of the domestic and industrial water
370 uses.

370

371 At monthly scale, GPP was increasing in all the months except July, August and
372 September (Fig.8). The positive trends were contributed principally by the summer harvest
373 crops (wheat as the main crop), while the negative trends were mainly contributed by the
374 autumn harvest crops (maize as the major crop). Regressive analysis showed that the
375 downward trends of GPP in summer season were resulted from the significant declines of
376 monthly sunshine duration and radiation ($r=0.38$ to 0.57 from June to August, $p < 0.05$).



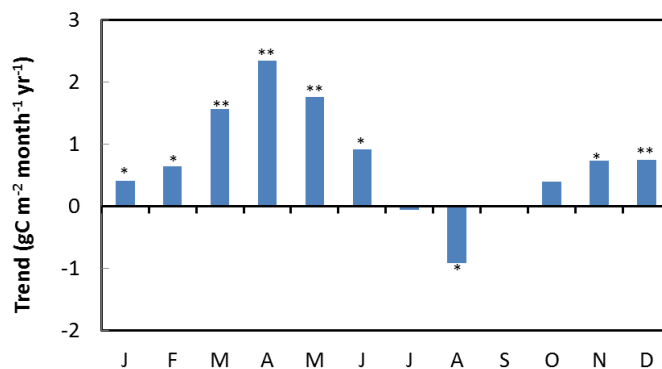
376



377

378 Fig.7 (a) Spatial distribution of GPP trends and (b) Pearson coefficients of trend at $p < 0.05$

379 significant level.



380

381

382 Fig.8 Monthly trend of GPP from 1981 to 2013 (Significant levels: * is $p < 0.05$; ** is $p < 0.01$).

383

384 3.2.3 Evapotranspiration (ET)

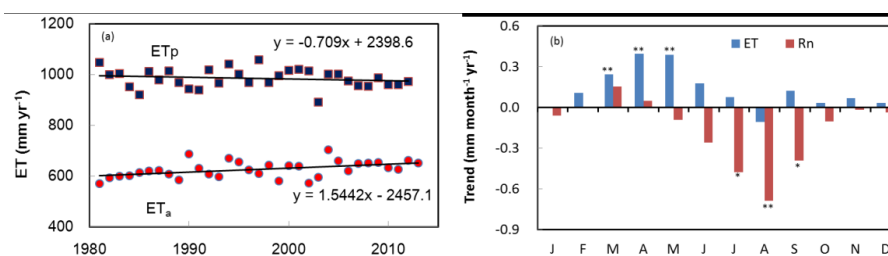
385 Water loss from the vegetation surface as ET is directly regulated by atmospheric vapor
386 demand and leaf stoma physiologically functioning (Buckley & Mott, 2013). Inter-annual
387 variation of ET is controlled by climate variability/change and agronomical managements.
388 Generally potential ET (ET_p) is used to represent the available energy for water vaporization
389 on land surface. As shown in Fig.8a, ET_p was slightly decreasing over the plain during the last
390 three decades, resulted from offsetting among the effects of reduced global radiation,
391 declining wind speed and increasing water vapor deficit (Song et al., 2009); simultaneously,



392 actual ET was predicted to be slightly increasing ($p < 0.05$), consistent with the enhancement
393 of greenness. It was noticed that the evolutions of potential and actual ET coincided with the
394 hypothesis of complementary relationship. At monthly scale, ET was significantly increasing
395 from February to April, but it was decreasing in August (Fig. 8b). This implicates that climate
396 warming may be beneficial to spring crops by waking wheat recovering early from dormancy,
397 whereas decline of net radiation (R_n) (especially in August, significant level $p < 0.001$) may
398 lead to the downward tendency of ET rates in summer.

399 Over the whole plain, spatially averaged actual ET and transpiration were 627 ± 162 mm
400 yr^{-1} (about 92% of annual precipitation) and 416 ± 129 mm yr^{-1} (about 67% of ET),
401 respectively. The trend of annual ET ($p < 0.1$) with CV (coefficient of variation) of 0.05 was
402 0.88 mm yr^{-2} from 1981 to 2013, which was less significant than that of NDVI ($p < 0.01$).
403 Decadal ET amounts in 1980s, 1990s and 2000s were 610, 626 and 640 mm, respectively,
404 corresponding to the slightly rising trend of precipitation. It is found that GPP increased with
405 higher significant level than that of ET, implicating the enhancement of water productivity in
406 the plain. Spatially, the trends of ET were positive over 86.0% of the study region,
407 distinguishing in the mid and southern parts, while negative trends were mostly occurred in
408 the northern part (Fig. 9(a, b)), which was consistent with the pattern of GPP tendencies. By
409 using a water balance model, Zeng et al. (2014) also presented an increasing trend of ET over
410 the North China Plain from 1982 to 2009.

411

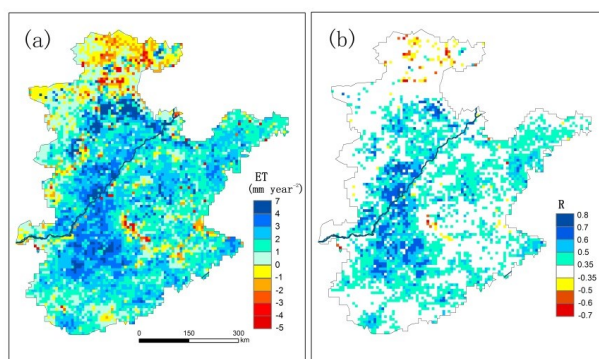


412

413

414 Fig.9 Inter-annual trends of potential and actual annual ET (a) and trends of monthly ET
415 and net radiation (R_n) (b) from 1981 to 2013 (Significant levels: * is $p < 0.05$; ** is $p < 0.01$).

416



417

418 Fig.10 (a) Spatial distributions of ET trends, and (b) their temporal Pearson coefficients
419 above $p < 0.05$ significant level from 1981 to 2013.

420

421 3.3 Contributions of climate change, atmospheric CO₂ fertilization and 422 agronomical management to changes of ET and GPP

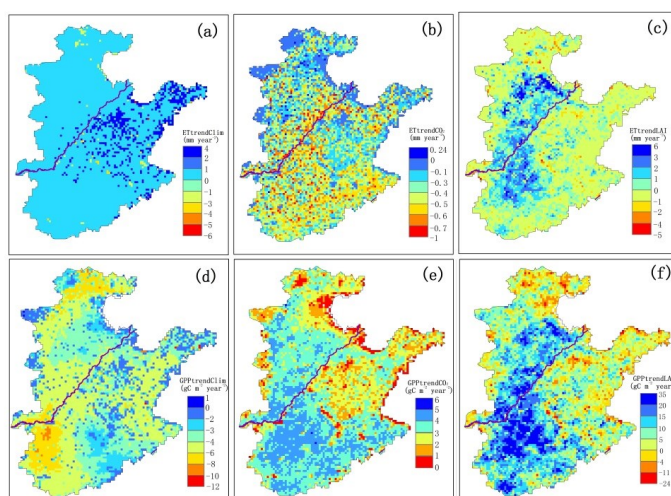
423 3.3.1 Spatial patterns of the contributions

424 The contributions from climate change, atmosphere CO₂ enrichment fertilization and
425 agronomical management illustrated considerably spatial heterogeneity for both ET and GPP
426 (Fig.11). Over the whole plain, climate change was exerting positive impact on water vapor
427 exchange from land surface to the atmosphere (f_i), especially in the eastern hilly part where
428 precipitation was increasing slightly. As general knowledge, air CO₂ enrichment stimulates
429 the crop leaf stomatal closing and then reduces transpiration, but its fertilization effect
430 enhances photosynthetic rate and water use efficiency (Buckley and Mott, 2013).
431 Descriptions of the separated effects were presented as following:

432 The climate change has intensified ET rate almost in the whole area, resulting in 0 to 4 mm
433 increment per year. The effect of climate change was much stronger in the mid to eastern
434 zones with high crop productivities, contributed mainly by air temperature increasing. The
435 contribution of CO₂ enrichment on ET is negative in most areas, ranging from 0 to -1 mm per
436 year. The attributions of agronomical practices and technological advancement represented by
437 LAI increase are somewhat complex, namely remarkable increase ranged from 0 to 6 mm per



438 year in the mid-western area where irrigation facilities and soil conditions have been
 439 ameliorated greatly in the recent decades through land consolidation, de-salinization. Renewal
 440 of cultivars and improved agronomical practices also contributed to the ET intensifying
 441 (Zhang et al., 2011). On the contrary, the grids with expansions of built-ups contributed to
 442 negative trends of ET, relating to urbanization and land use changes.



443

444

445 Fig.11 Contributions of climate changes, CO₂ enrichment and management on ET (a, b, c) and
 446 GPP (d, e, f) respectively (a and d are for climate; c and e for CO₂; c and f are for
 447 management)

448

449 Annually, contribution of climate change to GPP is negative, ranged from 0 to -12 gC m⁻²
 450 per year. Lower rates were occurred in the southwestern and northern parts. Air warming and
 451 heat waves, declines of precipitation and global radiation are the main causes of crop
 452 production reduction (Lobell et al., 2011; Guo et al., 2014). In addition, the spatial variability
 453 of climate change effects are associated with the relevant land use/cover and cropping
 454 systems. In the hilly areas (western and mid) and eastern coast areas, negative effects were
 455 slight, where air warming and air pollution were relatively weak. CO₂ enrichment effects
 456 were positive over the whole plain, ranged from 0 to 6 gC m⁻² per year. It was noticed that the
 457 higher effects were associated with higher cropland with favourable irrigation and high
 458 productivity, while the lower rate was related with low productivity croplands and natural
 459 vegetation communities. Similarly, the effects of human activities on ET were positive in the



460 mid to western areas, ranging from 0 to 35 gC m⁻² per year, associated with croplands of high
461 productivity. The negative effects were mainly occurred in the eastern and northern parts
462 where there is remarkable expansion of urban and dwelling built-ups in the study period.

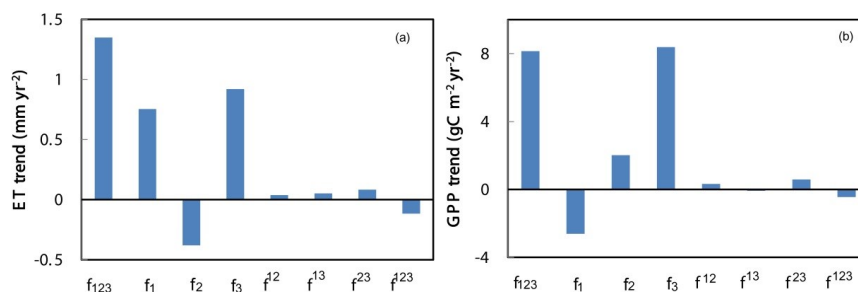
463 3.3.2 Regional averaged contributions

464 On the aspect of regional average, some characteristics of the contributions to water and
465 carbon assimilation are revealed. As shown in Fig.12(a), the contributions of climatic variable
466 change (f_1), elevated atmospheric CO₂ concentration (f_2) and agronomical management
467 (represented by leaf area index (LAI) increment) (f_3) and their interactions to the long term
468 trend of ET were positive, while the contribution of elevated atmospheric CO₂ is negative in
469 the last three decades. It was shown that the contribution of climate change was less than that
470 of agronomical improvement. The relative direct contributions of climatic change, CO₂
471 fertilization and agronomical management and technologic advancement to
472 evapotranspiration long term trend are 56, -28 and 68%, respectively. Compared with the
473 contributions of direct effects, the relative contributions by their interactions were low (the
474 cumulative effect of f^{A2} , f^{A3} , f^{23} and f^{A23} was only about 4%). Although the global radiation
475 reaching ground was diminished by higher aerosol concentration and deteriorated pollution in
476 the atmosphere (Che et al., 2005), its negative effect on terrestrial ET was offset by the
477 positive effects of air warming and higher vapor pressure deficit (VPD) on ET at annual scale.
478 Reduction of transpiration by enriched atmospheric CO₂ caused by closure of plant leaf
479 stomata at high CO₂ concentration for both C3 and C4 plants may mediated the extra water
480 demand by air warming. The dominant contribution was from the renewal of cultivars and
481 improvement of agricultural techniques and management. In the study period, agronomical
482 management has greatly improved, including the establishment of irrigation facility, prevalent
483 uses of chemical fertilizers and pesticides. For example, irrigated area in the northern part
484 (mainly Hebei Plain) has increased by 2.5 times, and chemical synthetic fertilizer input has
485 increased about four times, consequently, crop grain production has enhanced about two times
486 from 1980s to 2000s(Xu et al., 2005). Climate change and management improvement
487 (Irrigation practice, synthetic fertilizers supply and new cultivars adoption) are the main



488 contributors of ET intensifying over the plain.

489 As shown in Fig.12(b), the enriched atmospheric CO₂ fertilization and agronomical
490 management improvement presented a positive contribution to GPP trend during the study
491 period. It was somewhat out of expectation that the contribution of climate change to GPP
492 was negative at annual scale. The relative contributions of climate change, CO₂ fertilization
493 and management to the vegetation GPP enhancement were -32, 25 and 103%, respectively,
494 which demonstrated that the improvement of agricultural management was the dominant
495 driver to GPP increasing in recent decades. The positive effects on GPP were associated with
496 human activities and natural factors, such as input of synthetic fertilizers and atmospheric
497 nitrogen deposition, irrigation and other agronomical technology improvement, as well as
498 fertilization of enriched atmospheric CO₂. The negative contribution by climate change was
499 mainly happened in summertime (Fig.8). Since there was less benefit of CO₂ enrichment to
500 summer maize (C4 type), the reduced maize productivity due to global radiation decline was
501 not fully offset. Some researches, such as Piao et al. (2015) also reported that climate change
502 was exerting negative impact on the vegetation greening trend in the northern part of NCP
503 (including Hebei, Beijing, Tianjin Districts); Liu et al. (2010) attributed the reduction of crop
504 productivity over the NCP to shortening of vegetative growth length under climate warming.
505 As shown in Fig.4b, it was illustrated by NDVI time series that greenness in summer season
506 was quite stable; however it is significantly increasing in spring and autumn seasons,
507 indicating that climate warming was beneficial for crop growing in the cool seasons. In
508 addition, carbon assimilated by summer crops was larger than that in spring. Thereby, the sign
509 of GPP annual trend was determined by the trend in summer season. As air temperature
510 increasing was not so detrimental to maize growth in summer season yet, the decline of
511 downward shortwave radiation was considered to be responsible for GPP decline.



512

513

514 Fig.12(a) Contributions of climate change, atmospheric CO₂ enrichment and agronomical
515 management to ET and (b) contributions to GPP trends

516

517 3.3.3 Effects of climatic variables on monthly ET and GPP trends

518 To attribute the responses of cropping systems to the trends of single climatic variables,
519 the VIP model is used to diagnose the effects of climate change on ET and GPP at Beijing
520 meteorological observation site. The contributions of a single variable to the trends of ET and
521 GPP are expressed by their differences simulated with the current and de-trended variables
522 respectively. Here only the climatic variables of radiation, air temperature and wind speed are
523 linearly de-trended at monthly scale, since no significant trends of precipitation and humidity
524 are detected. As shown in Table 2, while the global radiation was de-trended, the negative
525 correlation coefficient of monthly GPP with time was reversed from negative to positive in
526 springtime, and from significant ($r < -0.6$, $p < 0.01$) to insignificant levels ($r < -0.15$, $p > 0.01$) in
527 July and August. It was affirmed that the decline of global radiation was the dominant factor
528 for reduction of crop GPP in summer period (June to August), but in autumn season the
529 changes of radiation, temperature and wind speed were all responsible for GPP changes. From
530 Table 2, it could be deduced that the effects of temperature rising on crop productivity was
531 positive and significant in spring (March and April) and autumn (September and October),
532 whereas its effect was weak in summer (May to August). It was noticed that the effect of
533 radiation change was quite weak in March, when no significant trend of shortwave radiation
534 was detected. In spring season sunshine durations were increasing from 1980s to 2010s
535 (Wang and Yang, 2014). In June, except global radiation, changes of temperature and



536 precipitation have contributed to GPP increasing. Additionally, fertilizing effect of enriched
537 CO₂ on C3 crop is a critical driver to GPP increasing. However, since the maize as C4 crop
538 does not benefit much from atmospheric CO₂ enrichment, new cultivars with higher light use
539 efficiency should be adopted to sustain the maize productivity under declined global radiation
540 condition resulted from exacerbating aerosol concentration and air pollutions.

541 Comparatively, the effect of climatic change on ET was less significant than that of
542 vegetation GPP. The model simulations showed that ET enhanced by air temperature rising
543 was mainly occurring in August to October, while the effect of solar radiation decreasing was
544 detected from June to September in the maize growing period.

545

546 Table 2 Monthly Pearson correlation coefficients of GPP trends (r_{ALL}: all variable are not
547 de-trended; r_R: radiation is de-trended; r_T: air temperature is de-trended; r_{R-T-U}:
548 radiation, temperature (T) and wind speed (U) are all de-trended).

	Jan	Feb	Mar	Apr	May	Jun	Jul	Aug	Sep	Oct	Nov	Dec
r _{ALL}	0.17	0.14	0.36	0.31	0.25	-0.16	-0.56	-0.37	-0.75	-0.48	-0.19	-0.03
r _R	0.29	0.15	0.38	0.40	0.23	0.49	-0.15	-0.07	-0.67	-0.46	-0.18	-0.03
r _T	0.11	-0.06	0.02	0.09	0.30	0.05	-0.64	-0.30	-0.48	0.08	0.08	0.05
r _{R-T-U}	0.10	-0.05	0.00	0.11	0.33	0.35	-0.20	-0.08	-0.13	0.10	0.09	0.06

549

550 4 Discussion

551 Our simulations suggested that annual ET and vegetation GPP were increasing over the
552 North China Plain during 1981 to 2013. Climate change contributed positive to ET
553 intensification, but it contributed negatively to GPP enhancement. Agronomical management
554 and technological advancement are the dominant factor to promote GPP increasing. The use
555 of remote sensing NDVI series have greatly improved the reliability of the vegetation water
556 consumption and productivity prediction at spatial and temporal scales, even if there were
557 uncertainty in vegetation characteristics retrievals from NDVI dataset. The results were
558 supported and consistent with most relevant studies at field and regional scales.

559 4.1 Is the trend of ET upward or downward over the NCP?

560 Although the crop productivities are steadily increasing, whether the actual ET over the
561 NCP is increasing or decreasing during the last three decades is controversial from the



562 reported literatures. By using the complementary relationship models (Brutsaert and Stricker,
563 1979), actual ET and potential ET both were decreasing (Cao et al., 2014; Gao et al., 2011).
564 However, ET was increasing predicted by the process - based VIP model from 1981 to 2013,
565 which was in consistent with the increasing trend of terrestrial greenness (Wang et al., 2016).
566 Yuan and Shen (2013) found that in the Northern part of NCP (Hebei Province) ET was
567 positively correlated with crop grain yield and agricultural water use was increasing from
568 2004 to 2008. Field measurements under well - watered fields also showed that seasonal ET
569 rates of both winter wheat and summer maize were increasing (Zhang et al., 2011). Brutsaert
570 (2006) acknowledged that decreasing pan evaporation was an evidence of increasing
571 terrestrial evaporation. As general knowledge, the sign of ET change should be the same as
572 that of vegetation greenness. Over the NCP a positive trend of ET was more believable, in the
573 light of significantly increasing NDVI over the growing season, especially in spring. The
574 positive effects of warming with higher water vapor deficit on ET might be offset by the
575 negative effect of declining solar radiation and wind speed on potential evaporation. On
576 viewpoint of the complementary relationship hypothesis (Hobbins et al., 2001), alteration of
577 available energy partitioned into latent heat flux (or ET) is dominated by the atmospheric
578 water vapor deficit. Namely, while more vapor is evaporated into the atmosphere boundary
579 layer, its water vapor deficit is correspondently relaxed, resulting in a lower rate of ET_p .
580 However, while declining global radiation being the dominant factor to ET trend, actual ET
581 (ET_a), wet surface ET (ET_w) and potential ET (ET_p) are all tracing the trend of available
582 energy (net radiation). In the study period, net radiation was declining with a rate of -5.58 MJ
583 yr^{-1} ($r=0.56$, $p<0.01$) over the NCP. As the trends of both ET_p and ET_w were dominated by the
584 radiation trend in the NCP, then ET_a estimated from the complementary relationship was
585 definitely following the negative trend of radiation, because the positive trend of aerodynamic
586 evaporation was weak as a tradeoff of positive effect of rising water vapor deficit and
587 negative effect of decreasing wind speed. However, the declining ET trend resulted from the
588 reduced radiation has actually been reversed by increasing green leaf area, which would
589 reduce land surface albedo and temperature, etc. Consequently, ET and GPP were showing
590 slightly increasing. This study case also confirmed the limitations of the complementary
591 relationship for assessment of evaporation trend under the condition of radiation declining.



592 **4.2 Effects of climate change and CO₂ on the cropping systems**

593 Without adaptation measures, climate change is illustrated to exert negative effects on the
594 productivity of cropping system in the NCP during the last three decades (Mo et al., 2013; Liu et
595 al, 2010). Changes of individual climate variables affected differently on specific cropping
596 systems, associated with crop type and growing season. Climate warming in winter and spring
597 seasons was benefit to vegetative growth of winter wheat (Mo et al., 2013). Although air warming
598 has shortened the growing length, the autonomously adopted cultivars with higher thermal
599 requirement usually maintained the crop growth length and accumulated more photosynthesis
600 product, which may outweigh the extra respiration consumption under warmer climate (Wang et
601 al., 2010). So far as, the effects of global warming on wheat production were inhomogeneous in
602 the North China Plain, which were positive in the northern part but negative in the southern part
603 (Zhang et al., 2013). The reasons are that during the wheat growth period air temperature is still
604 below the favorable conditions in the high latitude part of the plain, thereby recent global warming
605 is benign to the wheat growth, however, the air warming may be detrimental in the southern part,
606 especially for rainfed wheat (Xiao and Tao, 2014).

607 However, dominated by summer monsoon in the North China Plain, climate is hot in summer
608 maize growth period. Due to maize is tropical originated species with high thermal requirement, it
609 can tolerate relative high air temperatures. Our study showed that it was not suffered noticeably
610 from air warming in the recent decades, confirmed also by Xiong et al. (2012). However Guo et al.
611 (2014) reported that effect of air warming on maize was adverse with an Agro-Ecological Zones
612 model and the decreased daily temperature range (DTR) may be detrimental to crop yields.
613 Currently, adaptation measures may boost the production, such as harvest time delay (Wang et al.,
614 2014) or planting date advancement (Sacks and Kucharick, 2011) .

615 As increase of atmospheric aerosols by industrial production and combustion, global
616 radiation has declined in many parts of the world, in which direct component decreased but diffuse
617 component increased, so called “global dimming” (Liepert, 2002; Ren et al., 2013). The decline of
618 global radiation has resulted in less pan evaporation and carbon assimilation in crop and natural
619 vegetation communities (Xiong et al., 2012; Xiao and Tao, 2014), nevertheless plant canopies can
620 use the diffuse radiation with higher efficiency than direct beam (Gu et al., 2002). In spring time,
621 while the atmospheric circulation is shifting from continental to ocean monsoon in East Asia, the



622 wind speed is relative high and consequently air pollution and aerosols are usually low, thereby
623 global radiation is not reduced obviously in the wheat growth period (Table 1), illustrating that air
624 warming and precipitation variability other than radiation decrease are the principal climate
625 factors contributing to the tendency of wheat production. In contrast, global radiation decline
626 significantly in summer season in the North China Plain (Table 1), as a result, productivities of
627 autumn harvest crops such as maize are mainly affected. For example, Guo et al. (2014) reported
628 that maize potential productivity was reduced by 20 kg hm^{-2} due to global radiation decline in the
629 last decades over China.

630 During the study period of 1981 to 2013, atmospheric CO_2 concentration increased from
631 340 to 396 ppm, which contributed to enhancement of crop productivity. However, most studies
632 with statistical analysis models neglected the contribution of CO_2 fertilization (e.g., Lobell and
633 Burke, 2010; Song et al., 2014). As confirmed by FACE experiments, elevated atmospheric CO_2
634 concentration is accelerating plant photosynthesis and reducing transpiration, whose fertilizer
635 effect is 0.065% per ppm increase for C3 plants (Field et al., 1995; Long et al., 2006; Ainsworth et
636 al., 2008). In our simulations, the contribution of CO_2 to GPP was positive while to ET was
637 negative. The positive CO_2 effect on GPP almost compensates for the negative effects of climatic
638 variable changes. However, we should bear in mind, as Ainsworth et al. (2008) pointed out that the
639 CO_2 fertilizer effect may be over-estimated by the process-based crop/ecosystem models.

640 **4.3 Effects of agronomical practice and technique advancement and other** 641 **factors**

642 Remotely sensed NDVI is an excellent indicator for long term changes of vegetation covers.
643 Here we assumed that climate change did not modify the tendencies of vegetation covers, but
644 dominated its inter-annual variation. Renewal of crop cultivars, applications of synthetic fertilizer
645 and irrigation, as well as conservancy tillage and nitrogen deposition are all contributing to the
646 crop and/or natural productivity improvements (Yu et al., 2012; Bai et al., 2015; Piao et al., 2015).
647 National statistical records of grain yields at county scale showed rapid increase from 1980 to
648 1990, and moderate increase in 2000s. Enhancement of crop yields was mainly stemmed from
649 more biomass accumulation and higher harvest index than previous varieties (Zhang X. et al.,
650 2013). In our simulations the upward trend of GPP was more significant than that of ET, which
651 was in consistent with the increasing trend of cumulative NDVI. Agronomical practices and



652 technology advancement contributed to 103% GPP changes in our study. By using crop models,
653 Yu et al. (2012) and Song et al. (2014) reported relative contributions of 92% and 62% by
654 agronomical management and renewal of cultivars for rice respectively, and Guo et al. (2014)
655 presented that 99.6 to 141.6% maize yield increases was contributed by technological
656 advancement in China since 1980s. The previous studies showed, if no adoption measures were
657 taken, climate change generally contributed negatively to crop productivities in the mid-latitude
658 areas, but the negative effects were usually compensated for by genetic improvements,
659 applications of fertilizer and irrigation, pest and weed control, as well as CO₂ and nitrogen
660 deposition effects (Liu et al., 2010; Lobell et al., 2011; Guo et al., 2014; Bai et al., 2015). Under
661 warming climate condition, it is expected that water requirement by crops and natural plants will
662 increase, but the intensified ET may be limited by insufficient soil moisture availability. Therefore,
663 the sustainability of crop productions are greatly depending on the improvement of agronomical
664 management and technological advancement on variety breeding.

665 **5. Summary and conclusions**

666 Climate change and human activities have greatly altered the hydrological regime and
667 crop productivity in the North China Plain with warm temperate climate during the recent
668 three decades. The VIP ecological model integrated the NOAA-AVHRR NDVI data series
669 predicted that spatial average annual actual ET was weakly increasing while vegetation
670 primary productivity (GPP) was significantly increasing ($p < 0.01$) from 1981 to 2013, being
671 consistent with remotely sensed NDVI trend. The increases of actual ET and GPP were
672 mainly occurred in spring season, while ET and GPP were obviously decreasing in August
673 owing to global radiation diminishing.

674 Climate change, elevated atmospheric CO₂ fertilization and agronomical management all
675 contributed to the inter-annual trends of ET and crop GPP. The relative direct contributions of
676 climatic change, CO₂ fertilization and agronomical management to ET increasing were 56,
677 -28 and 68%, while the contributions to GPP were -32, 25 and 103%, respectively. Air
678 warming intensifies the crop water requirement and enhances the production of crops
679 harvested in summer. The decline of global radiation resulted from exaggerated aerosol



680 concentration and air pollutions was considered to be the main cause of GPP reduction in
681 August. The study confirmed the necessary for imminent control of air pollution and aerosol
682 to sustain the agriculture system productivity.

683 **Acknowledgements**

684 This work was supported by the Natural Science Foundation of China grants (41471026
685 and 31171451). We thank the China Meteorological Administration (CMA) for providing the
686 meteorological data and on-site soil moisture data used in this paper.

687

688 **References**

- 689 Ainsworth, E. A., Leakey, A. D. B., Ort, D. R. and Long, S. P.: FACE-ing the facts:
690 inconsistencies and interdependence among field, chamber and modeling studies of
691 elevated [CO₂] impacts on crop yield and food supply, *New Phytol.*, 179, 5–9, 2008.
- 692 Alkama, R., Kageyama, M., Ramstein, G.: Relative contributions of climate change, stomatal
693 closure, and leaf area index changes to 20th and 21st century runoff change: A modelling
694 approach using the ORCHIDEE land surface model, *J. Geophys. Res.* 115, D17112, doi:
695 10.1029/2009JD013408, 2010.
- 696 Bai, H., Tao, F., Xiao, D., Liu, F. & Zhang, H.: Attribution of yield change for rice-wheat
697 rotation system in China to climate change, cultivars and agronomic management in the
698 past three decades, *Clim. Change*, DOI 10.1007/s10584-015-1579-8, 2015.
- 699 Banger, K., Tian, H., Tao, B., Ren, W., Pan, S., Dangal, S., Yang, J.: Terrestrial net primary
700 productivity in India during 1901–2010: contributions from multiple environmental changes,
701 *Clim. Change*, 132, 575–588, 2015.
- 702 Betts, R. A., et al.: Projected increase in continental runoff due to plant responses to increasing
703 carbon dioxide, *Nature*, 448, 1037–1041, 2007.
- 704 Brutsaert, W. B.: Indications of increasing land surface evaporation during the second half of the
705 20th century, *Geophys. Res. Lett.* 33, L20403, doi:10.1029/2006GL027532, 2006.
- 706 Brutsaert, W., Stricker, H.: An advection-aridity approach to estimate actual regional
707 evapotranspiration, *Water Resour. Res.* 15(2), 443–450, 1979.
- 708 Buckley, T.N. & Mott, K.: Modelling stomatal conductance in response to environmental factors,
709 *Plant Cell Environ.*, 36, 1691–1699, 2013.
- 710 Burn, D. H., Hesch, N. M.: Trends in evaporation for the Canadian Prairies, *J. Hydrol.*, 336, 61–
711 73, 2007.



- 712 Cao, G, Han, D. and Song, X.: Evaluating actual evapotranspiration and impacts of groundwater
713 storage change in the North China Plain, *Hydrol. Process.*, 28, 1797–1808, 2014.
- 714 Che, H.Z., Shi, G.Y., Zhang, X.Y., et al.: Analysis of 40 years of solar radiation data from China,
715 1961–2000, *Geophys. Res. Lett.* 32,1–5, 2005.
- 716 Chen L., Zhang, L., Wang Y., Yu, Q., Eamus, D., O’Grady, A.: Impacts of elevated CO₂, climate
717 change and their interactions on water budgets in four different catchments in Australia, *J.*
718 *Hydrol.*, 519, 1350-1361, 2014.
- 719 Cho, M.-H., Boo K.-O., Lee J., Cho C., and Lim G.-H.: Regional climate response to land surface
720 changes after harvest in the North China Plain under present and possible future climate
721 conditions, *J. Geophys. Res. Atmos.* 119, 4507–4520, doi:10.1002/ 2013JD020111, 2014.
- 722 Collatz, G. J., Ribas-Carbo, M., and Berry, J. A.: Coupled photosynthesis-stomatal conductance
723 model for leaves of C4 plants, *Aust. J. Plant Physiol.*, 19, 519–538, 1992.
- 724 Douville, H., Ribes, A., Decharme, B., Alkama, R. and Sheffield, J.: Anthropogenic influence
725 on multidecadal changes in reconstructed global evapotranspiration, *Nature-climate change*,
726 DOI: 10.1038/NCLIMATE1632, 2013.
- 727 Ewert, F., Rotter, R.P., Bindi, M., Webber, H., Trnka, M., et al.: Crop modelling for integrated
728 assessment of risk to food production from climate change, *Environ. Model. & Soft.*, 72,
729 287-303, 2015.
- 730 Farquhar, G. D., von Caemmerer, S., and Berry, J. A.: A biochemical model of photosynthetic
731 CO₂ assimilation in leaves of C3 species, *Planta* 149, 78–90, 1980.
- 732 Field, C., Jackson, R., and Mooney, H.: Stomatal responses to increased CO₂: Implications from
733 the plant to the global scale, *Plant Cell Environ.*, 18, 1214–1255, 1995.
- 734 Gao, G., Xu, C., Chen, D., Singh, V. P.: Spatial and temporal characteristics of actual
735 evapotranspiration over Haihe River basin in China, *Stoch Environ. Res. Risk Assess.*, 26,
736 655–669, 2012.
- 737 Gu, L. H., Baldocchi, D., Verma, S. B., Black, T. A., Vesala, T., Falge E. M., and Dowty, P. R.,:
738 Advantages of diffuse radiation for terrestrial ecosystem productivity, *J. Geophys.*
739 *Res.-Atmos.*, 107(D6), 4050, doi:10.1029/2001JD001242, 2002.
- 740 Guo, J., Zhao, J., Wu, D., Mu, J., Xu, Y.: Attribution of Maize Yield Increase in China to
741 Climate Change and Technological Advancement Between 1980 and 2010, *J. Meteorol.*
742 *Res.*, 28(6), 1168-1181, doi: 10.1007/s13351-014-4002-x, 2014.
- 743 Haddeland, I., Heinke J., Biemans H. et al.: Global water resources affected by human
744 interventions and climate change, *PNAS*, 111 (9), 3251–3256, 2014.
- 745 Hobbins, M. T., Ramirez J. A., Brown T. C., Claessens L. H. J. M.: The complementary
746 relationship in estimation of regional evapotranspiration: The Complementary Relationship
747 Areal Evapotranspiration and Advection-Aridity models, *Water Resour. Res.*, 37(5), 1367–
748 1387, 2001.



- 749 Hu, S., Mo X., Lin Z.: Optimizing the photosynthetic parameter V_{cmax} by assimilating
750 MODIS-fPAR and MODIS-NDVI with a process-based ecosystem model, *Agric. For.*
751 *Meteorol.*, 198–199, 320–334, 2014.
- 752 Katul, G. G., Oren R., Manzoni S., Higgins C., and Parlange M. B.: Evapotranspiration: A process
753 driving mass transport and energy exchange in the soil-plant-atmosphere-climate system, *Rev.*
754 *Geophys.*, 50, RG3002, doi:10.1029/2011RG000366, 2012.
- 755 Liepert, B.G.: Observed reductions of surface solar radiation at sites in the United States and
756 worldwide from 1961 to 1990, *Geophys. Res. Lett.*, 29, 61-1 – 61-4, 2002..
- 757 Liu, M., Tian H., Lu C., Xu X., Chen G., Ren W.: Effects of multiple environment stresses on
758 evapotranspiration and runoff over eastern China, *J. Hydrol.*, 426–427,39–54, 2012.
- 759 Liu, S., Xu, Z.: Multi-scale surface flux and meteorological elements observation dataset in the
760 Hai River Basin (Miyun site-automatic weather station). *Cold and Arid Regions Science Data*
761 *Center at Lanzhou*, doi:10.3972/haihe.001.2013.db, 2013.
- 762 Liu Y., Wang, E., Yang, X.: Contributions of climatic and crop varietal changes to crop
763 production in the North China Plain, since 1980s, *Global Change Biol.*, 16, 2287–2299, 2010.
- 764 Lobell,D.B., Burke, M.B.: On the use of statistical models to predict crop yield responses to
765 climate change, *Agric. For. Meteorol.* 150, 1443-1452, 2010.
- 766 Lobell, D.B., Schlenker,W., Costa-Roberts, J.: Climate trends and global crop production since
767 1980, *Science* 333,616–620, 2011.
- 768 Long, S. P., Ainsworth, E. A., Leakey, A. D. B., Nosberger, J. and Ort, D.: Food for thought:
769 lower-than-expected crop yield stimulation with rising CO₂ concentrations, *Science*, 312,
770 1918–21, 2006.
- 771 Mao, J., Shi, X., Thornton, P. E, Piao, S., Wang, X.: Causes of spring vegetation growth trends in
772 the northern mid–high latitudes from 1982 to 2004, *Environ. Res. Lett.*, 7, 014010, 2012.
- 773 Marshall, M., Funk C., Michaelsen, J.: Examining evapotranspiration trends in Africa, *Clim. Dyn.*
774 38,1849-1865, 2012.
- 775 Ministry of Water Resources of China (MWR): China water resources bulletin, Ministry of Water
776 Res. of China, Beijing, 2010 [Available at <http://www.mwr.gov.cn/>].
- 777 Mo, X., Liu, S., Meng, D.: Climate variability impacts on evapotranspiration and primary
778 productivity by assimilating remotely sensed data with a process-based model over Songhua
779 River Basin, *Int. J. Climatol.*, 34, 1945–1963, DOI: 10.1002/joc.3813, 2014.
- 780 Mo, X., Guo, R., Liu, S., Lin, Z., Hu, S.: Impacts of climate change on crop evapotranspiration
781 with ensemble GCM projections in the North China Plain, *Clim. Change*, 120, 299–312, DOI
782 10.1007/s10584-013-0823-3, 2013.
- 783 Mo, X., Liu, S., Lin, Z.: Evaluation of an ecosystem model for wheat-maize double cropping
784 system over the North China Plain, *Environ. Model & Soft* 32, 61-73, 2012.
- 785 Nemani, R.R., Keeling, C.D., Hashimoto, H. et al.: Climate-driven increases in global terrestrial



- 786 net primary production from 1982 to 1999, *Science* 300, 1560–1563, 2003.
- 787 Nayak, R. K., Patel N. R. and Dadhwal, V. K.: Inter-annual variability and climate control of
788 terrestrial net primary productivity over India, *Int. J. Climatol.*, 33, 132-142, 2013.
- 789 Ozdogan, M., and Salvucci, G. D.: Irrigation-induced changes in potential evapotranspiration in
790 southeastern Turkey: Test and application of Bouchet's complementary hypothesis, *Water*
791 *Resour. Res.*, 40, W04301, doi:10.1029/2003WR002822, 2004.
- 792 Pinzon, J. E., Tucker, C. J.: A Non-Stationary 1981–2012 AVHRR NDVI3g Time Series, *Remote*
793 *Sens.*, 6, 6929-6960, 2014.
- 794 Qian, T., Dai, A., Trenberth, K. E.: Hydroclimatic trends in the Mississippi River from 1948 to
795 2004. *J. Clim.* 20, 4599-4614, 2007.
- 796 Piao, S., Yin, G., Tan, J., Cheng, L., Huang, M., et al., 2015. Detection and attribution of
797 vegetation greening trend in China over the last 30 years. *Global Change Biol.*, doi:
798 10.1111/gcb.12795.
- 799 Sacks, W.J., Kucharik C. J.: Crop management and phenology trends in the U.S. Corn Belt:
800 Impacts on yields, evapotranspiration and energy balance, *Agric. For. Meteorol.*, 151, 882–
801 894, 2011.
- 802 Savitzky, A., Golay, M.J.E.: Smoothing and differentiation of data by simplified least squares
803 procedures, *Anal. Chem.*, 36, 1627–1639, 1964.
- 804 Shi, X., Mao, J., Thornton, P.E., Hoffman, F. M., Post, W. M.: The impact of climate, CO₂,
805 nitrogen deposition and land use change on simulated contemporary global river flow,
806 *Geophys. Res. Lett.*, 38, L08704, doi:10.1029/2011GL046773, 2011.
- 807 Song, Z.W., Zhang, H. L., Snyder, R. L., Anderson, F. E., and Chen, F.: Distribution and Trends in
808 Reference Evapotranspiration in the North China Plain, *J. Irrig. Drain. Eng.* 136(4), 240-247,
809 2010.
- 810 Song, Y., Wang, C., Ren, G.: The relative contribution of climate and cultivar renewal to
811 shaping rice yields in China since 1981, *Theor. Appl. Climatol.* 120(1-2), 1-9, DOI
812 10.1007/s00704-014-1089-z, 2014.
- 813 Stein, U., and Alpert P.: Factor separation in numerical simulations. *J. Atmos. Sci.* 50, 2105-2115,
814 1993.
- 815 Tang, B., Tong, L. , Kang, S., Zhang, L.: Impacts of climate variability on reference
816 evapotranspiration over 58 years in the Haihe river basin of north China, *Agric. Water*
817 *Manage.* 98, 1660–1670, 2011.
- 818 Tian, H., Lu, C., Chen, G., Xu X., Liu, M., Ren, W., Tao, B., Sun, G., Pan, S., Liu, J.: Climate and
819 land use controls over terrestrial water use efficiency in monsoon Asia, *Ecohydrol.* 4, 322–
820 340, 2011.
- 821 Veron, S.R., de Aballeyra, D., Lobell, D.B.: Impacts of precipitation and temperature on crop
822 yields in the Pampas, *Clim. Change*, 130, 235–245, 2015.



- 823 Wang, J., Wang, E., Yang, X., Zhang, F., Yin, H.: Increased yield potential of wheat-maize
824 cropping system in the North China Plain by climate change adaptation, *Clim. Change*, 113,
825 825-840, 2012.
- 826 Wang, S., Mo, X., Liu, S., Lin, Z., Hu, S.: Validation and trend analysis of ECV soil moisture data
827 on cropland in North China Plain during 1981–2010, *Int. J. Appl. Earth Obs.* 48, 110–121,
828 2016.
- 829 Wang, Z., Ye, T., Wang, J., Cheng, Z., Shi, P.: Contribution of climatic and technological
830 factors to crop yield: empirical evidence from late paddy rice in Hunan Province, China.
831 *Stoch. Environ. Res. Risk Assess.* DOI 10.1007/s00477-016-1215-9, 2016.
- 832 Wang, Y. W. and Yang, Y. H.: China's dimming and brightening: evidence, causes and
833 hydrological implications, *Ann. Geophys.*, 32, 41–55, 2014.
- 834 Xiao, D., Tao F.: Contributions of cultivars, management and climate change to winter wheat
835 yield in the North China Plain in the past three decades, *Europ. J. Agron.*, 52, 112-122, 2014.
- 836 Xiong, W., Holman, I., Lin, E. D., et al.: Untangling relative contributions of recent climate and
837 CO₂ trends to national cereal production in China, *Environ. Res. Lett.*, 7, 044014, 2012.
- 838 Xu, Y., Mo, X., Cai Y., Li, X.: Analysis on groundwater table drawdown by land use and the quest
839 for sustainable water use in the Hebei Plain in China, *Agric. Water Manage.*, 75, 38–53, 2005.
- 840 Yan, H., Yu Q., Zhu Z.-C., Myneni R. B., Yan H.-M., Wang S. Q., and Shugart, H. H.: Diagnostic
841 analysis of interannual variation of global land evapotranspiration over 1982–2011:
842 Assessing the impact of ENSO, *J. Geophys. Res. Atmos.*, 118, 8969–8983,
843 doi:10.1002/jgrd.50693, 2013.
- 844 Yu, Y., Huang, Y., Zhang, W.: Changes in rice yields in China since 1980 associated with cultivar
845 improvement, climate and crop management. Changes in rice yields in China since 1980
846 associated with cultivar improvement, climate and crop management, *Field Crops Res.*, 136,
847 65–75, 2012.
- 848 Yuan, Z., Shen, Y., 2013. Estimation of agricultural water consumption from meteorological and
849 yield data: A case study of Hebei, North China, *PLoS ONE* 8(3): e558685.
850 Doi:10.1371/journal.pone.008685, 2013.
- 851 Zeng, Z. Z., Wang, T., Zhou, F., Ciais, P., Mao, J. F., Shi, X. Y., and Piao, S. L.: A worldwide
852 analysis of spatiotemporal changes in water balance-based evapotranspiration from 1982 to
853 2009, *J. Geophys. Res. Atmos.* 119, 1186–1202, doi:10.1002/2013JD020941.
- 854 Zhang, X., Chen, S., Sun, H., Shao, L., Wang, Y.: Changes in evapotranspiration over irrigated
855 winter wheat and maize in North China Plain over three decades, *Agric. Water Manage.*,
856 98, 1097–1104, 2011
- 857 Zhang, X., Wang, S., Sun, H., Chen, S., Shao, L., Liu, X.: Contribution of cultivar, fertilizer and
858 weather to yield variation of winter wheat over three decades: A case study in the North
859 China Plain, *Europ. J. Agron.*, 50, 52– 59, 2013.